Check for updates

ACES Asian Chemical Editorial Society

doi.org/10.1002/asia.202300681

CHEMISTRY AN ASIAN JOURNAL Research Article

www.chemasianj.org

New Molecular Design, Step-Saving Synthesis, and Applications of Indolocarbazole Core-Based Oligo(hetero)arenes

Li Lin,[a] Wei-Hao Chiu,[b] Ming-Ling Cao,[a] Kun-Mu Lee,*[b, c] Wei-Lun Yu,[a] and Ching-Yuan Liu*[a]

In this work, we have successfully synthesized 15 new examples (**LLA01-06**; **LinLi01-10**) of small-molecule hole-transporting materials (HTM) using the less explored indolocarbazole (ICbz) as core moiety. Different from previously reported ICbz HTMs, **LinLi01-10** exhibit new molecular designs in which 3,4-ethylenedioxythiophene (EDOT) units are inserted as crucial π-spacers and fluorine atoms are introdcued into end-group molecules. These substantially improve the materials solubility and device power conversion efficiencies (PCEs) while fabricated in perovskite solar cells (PSC). More importantly, **LinLi01-10** are generated by a sustainable synthetic approach involving the use of straightforward C–H/C–Br couplings as key transformations, thus avoiding additional synthetic transformations including halogenation and borylation reactions called *substrate prefunctionalizations* usually required in Suzuki reactions. Most HTM molecules can be purified simply by reprecipitations instead of conducting column chromatography. In contrast to **LLA01-06** without additional EDOT moieties, PSC devices using **LinLi01-10** as hole-transport layers display promising PCEs of up to 17.5%. Interestingly, PSC devices employing seven of the **LinLi01-10** as hole-transport molecules, respectively, are all able to show an immediate >10% PCE (t=0) without any device oxidation/aging process that is necessary for the commercial **spiro-OMeTAD** based PSCs.

Introduction

Both of indole and carbazole have been regarded as prominent building blocks in the fields of synthetic organic chemistry, medicinal chemistry, or organic semiconducting materials.[1–4] To capture the advantages from both molecules, their merged structure with a longer π-conjugation was created and called indolocarbazole (ICbz). ICbz has been extensively investigated in biochemistry-related areas since its molecular structure was characterized for the first time in Staurosporine, an alkaloid isolated from the bacterium named *streptomyces staurosporeus*.[5] Compared to the medicinal and pharmaceutical reports on ICbz-based molecules disclosed up to date, its synthesis and applications in π-conjugated optoelectronic materials were much less explored. Since ICbz exhibits rich π-electrons and high planarity, a number of research teams described the use of indolocarbazole as core functional molecule for the device fabrication of organic field-effect transistors (OFET),[6–8] dye-sensitized solar cells (DSSC),[9–10] or organic light-emitting diodes (OLED),[11] respectively. In addition, Yu/Yang[12] and Nazeeruddin[13] reported high-efficiency perovskite solar cells (PSC) utilizing ICbz-based small molecules as hole-transporting materials (HTM). Hence, in light of some impressive PSC-relevant papers and our recent research experiences and achievements in HTMs/PSCs,[14–19] we decided to design and synthesize a series of ICbz core-based new oligoaryls, as shown in Figure 1, HTMs **LLA01-06** and **LinLi01-10** with additional π-spacers were efficiently prepared and their power conversion efficiencies (PCEs) were comparably demonstrated while fabricated in PSC devices.

Results and Discussion

In Table 1, we demonstrated the synthesis of **LLA01-06** by performing Buchwald-Hartwig aminations of a dibromo- indolocarbazole derivative **1** with various diarylamines **2a–f** (we failed to obtain the analytically valid **2e** due to the formation of regioisomeric fluoro-containing carbazoles, thus the synthesis of **LLA05** was not carried out). Nevertheless, other expected products were successfully prepared under a typical amination reaction conditions, affording **LLA01**, **LLA02**, **LLA03**, **LLA04**, and **LLA06** in moderate to good isolated yields (58–85%).

Next, as shown in Scheme 1 regarding the preparation of **LinLi01-10** incorporating additional EDOT moieties as π-spacers, the step-saving synthetic route was carried out utilizing [Pd]-catalyzed direct C–H/C–Br cross-couplings as key transformations, which was compared to the multi-step synthesis requiring

[a] L. Lin, M.-L. Cao, W.-L. Yu, Prof. Dr. C.-Y. Liu
Department of Chemical and Materials Engineering
National Central University
Jhongli District, Taoyuan City 320 (Taiwan)
E-mail: cyliu0312@ncu.edu.tw

[b] Dr. W.-H. Chiu, Prof. Dr. K.-M. Lee
Department of Chemical and Materials Engineering & Center for Green Technology & Division of Neonatology, Department of Pediatrics
Chang Gung University & Chang Gung Memorial Hospital, Guishan District and Linkou, Taoyuan City 333 (Taiwan)

[c] Prof. Dr. K.-M. Lee
College of Environment and Resources, Ming Chi University of Technology, New Taipei City 243 (Taiwan)

Supporting information for this article is available on the WWW under https://doi.org/10.1002/asia.202300681

© 2023 Wiley-VCH GmbH

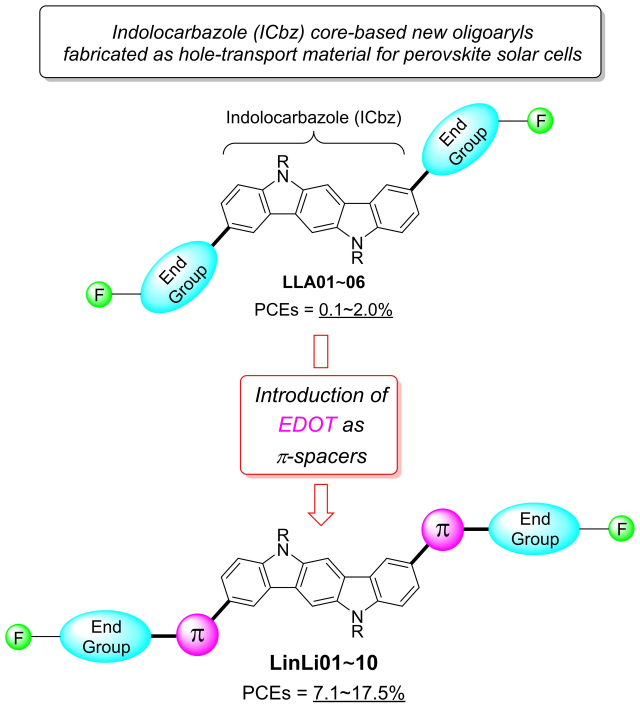

Figure 1. Indolocarbazole (ICbz) core-based new HTMs: **LLA01-06** *vs.* **LinLi01-10**. Introduction of EDOT as π-spacers significantly enhanced the PCEs of **LinLi01-10**-based perovskite solar cells.

prefunctionalization operations including Br/Li-exchange, borylation, and bromination for subsequent Suzuki reactions.

Accordingly, the efficient synthesis of **LinLi01-10** were successfully realized by the treatment of **1** with various end-groups **3a–j** under optimized C–H/C–Br coupling reaction conditions.[20] The results were summarized in Table 2. It was found that **3a** underwent direct C–H arylation smoothly with **1** to give **LinLi01** in moderate isolated yield (65%), whereas the sulfur congener (**3b**) was shown to be much less effective in present coupling reactions, producing **LinLi02** in only 14%. We reasoned that the poor conversion might result from the coordination of the $-S(CH_3)$ group to palladium complex, thus reducing the reactivity of [Pd]-based catalyst. We then investigated the end-groups bearing fluoro- or trifluoromethyl substituents (**3c–g**) and the desired products were readily obtained (**LinLi03-07**, 50–73%). It is worth noting that, compared to non-fluorinated ones, **LinLi03-07** exhibited relatively superior solubility in common organic solvents such as ethyl acetate, dichloromethane, tetrahydrofuran, or chlorobenzene for device fabrications. We think the introduction –F or $-CF_3$ moieties into LinLi03-07 considerably enhanced their lipophilicity. Besides triphenylamine derivatives (**3a–g**), we also examined carbazole (**3h**, **3i**)- and phenothiazine (**3j**)-based end-groups. The corresponding **LinLi08-10** were isolated in 37–71% yields. We found that, among all synthesized molecules demonstrated in Table 2, **LinLi08** possessed the poorest solubility, thus leading to difficulties in the purification step. In summary, the solubility order of our newly synthesized HTMs: **LinLi03-07** > **LinLi01/02** > **LinLi10** > **LinLi08/09** ≈ **LLA01-06**. In

Table 1. Synthesis of **LLA01-06** (except **LLA05**) by the Buchwald-Hartwig amination of **1** with **2a**, **2b**, **2c**, **2d**, or **2f**.[a, b]

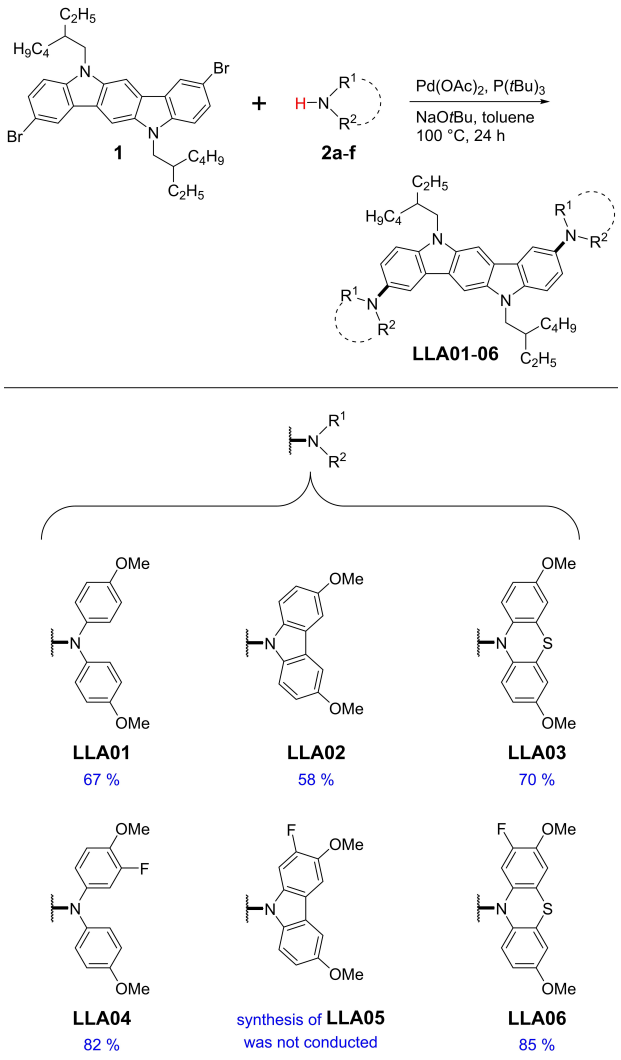

[a] Unless specified, amination reactions were conducted with **1** (1.00 mmol) and **2a-f** (except **2e**, 2.10 mmol) under N_2 in the presence of $Pd(OAc)_2$ (5 mol%), $P(t\text{-}Bu)_3$ (10 mol%), and NaO*t*Bu (3.00 equiv.) in toluene (3 mL) at 100 °C for 24 h. [b] Isolated yields.

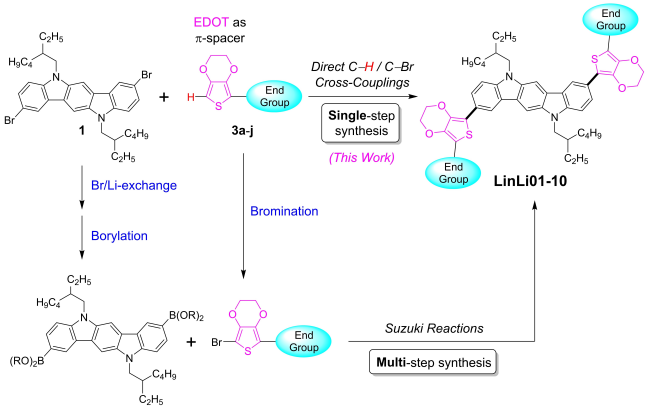

Scheme 1. Two synthetic routes to **LinLi01-10** involving EDOT as π-spacers: key steps using direct C–H/C–Br couplings or Suzuki reactions.

© 2023 Wiley-VCH GmbH

1861471x, 2023, 20, Downloaded from https://onlinelibrary.wiley.com/doi/10.1002/asia.202300681 by Ruhr-Universität Bochum, Wiley Online Library on [27/11/2023]. See the Terms and Conditions (https://onlinelibrary.wiley.com/terms-and-conditions) on Wiley Online Library for rules of use; OA articles are governed by the applicable Creative Commons License

Table 2. Synthesis of **LinLi01-10** by the direct C-H arylation of **3a-j** with **1**.[a, b]

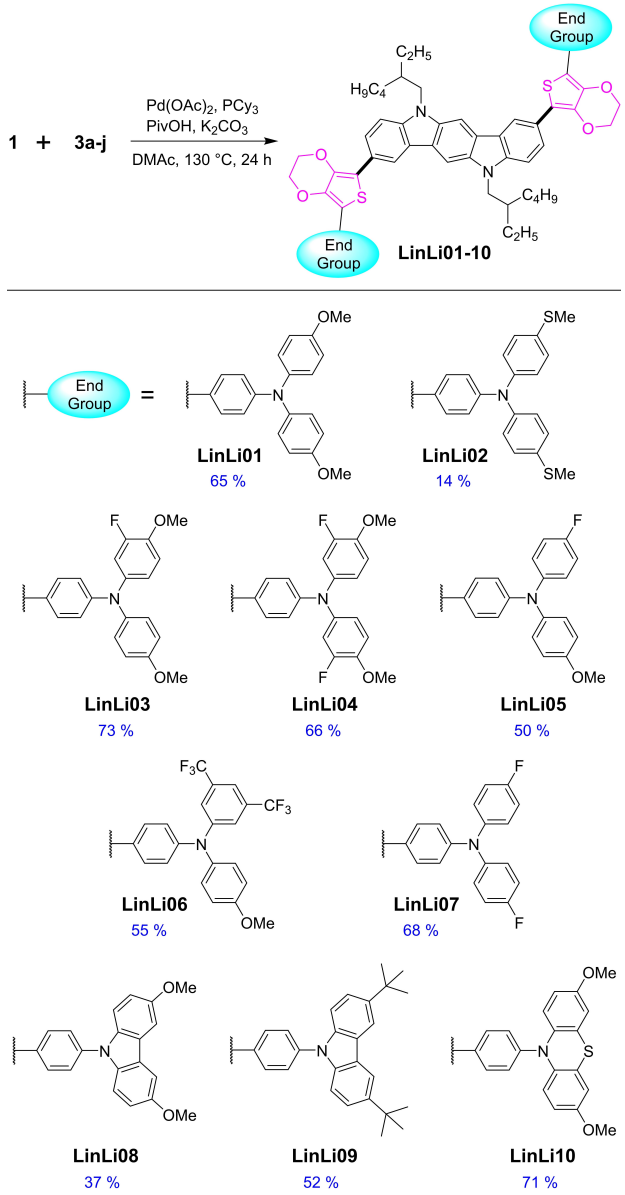

[a] Unless specified, the direct C–H/C–Br coupling reactions were conducted with **1** (1.00 mmol) and **3a–j** (2.10 mmol) under N_2 in the presence of $Pd(OAc)_2$ (10 mol%), $P(Cy)_3$ (20 mol%), PivOH (60 mol%), and K_2CO_3 (3.00 equiv.) in DMAc (3 mL) at 130 °C for 24 h. [b] Isolated yields.

Table 3. Summary of the optical-, electrochemical-, thermal-, and electrical properties of **LinLi01-10**.

HTMs	ΔE_g^{opt} [eV][a, b]	E_{HOMO} [eV][c]	E_{LUMO} [eV][d]	T_d [°C]	hole mobility [$cm^2V^{-1}s^{-1}$]
LinLi01	2.67	−5.17	−2.50	381	4.02×10^{-4}
LinLi02	2.53	−5.13	−2.60	382	5.47×10^{-4}
LinLi03	2.68	−5.21	−2.53	367	5.02×10^{-4}
LinLi04	2.70	−5.24	−2.54	332	6.08×10^{-4}
LinLi05	2.74	−5.23	−2.49	383	3.44×10^{-4}
LinLi06	2.70	−5.29	−2.59	368	4.23×10^{-4}
LinLi07	2.71	−5.24	−2.53	391	3.27×10^{-4}
LinLi08	2.73	−5.30	−2.57	390	4.84×10^{-4}
LinLi09	2.73	−5.33	−2.60	389	5.01×10^{-4}
LinLi10	2.67	−5.19	−2.52	389	3.35×10^{-4}

[a] UV–vis absorption and photoluminescence spectra were measured in dichloromethane solution. [b] ΔE_g^{opt} was calculated from the absorption onset of UV–vis spectra, $E_g^{opt}=1240/\lambda_{onset}$. [c] $E_{HOMO}=-(E_{ox,\ onset\ (vs.\ Fc/Fc+)}+5.16)$ eV. [d] $E_{LUMO}=E_{HOMO}+\Delta E_g^{opt}$.

addition, it is noteworthy that most products shown above (except **LinLi02**&**04**) can be obtained in high purity simply by reprecipitations from dichloromethane/hexanes, instead of conducting column chromatography.

For the EDOT-incorporated **LinLi01-10**, we investigated their optical-, electrochemical-, thermal stability- and hole mobility-characteristics. The results were collected in Table 3. First, Concerning the structure-property relationship between the donor ability (TPA: triphenylamine, Cbz: carbazole, and PTZ: phenothiazine) and the optical property (ΔE_g^{opt} and E_{HOMO}), we focused on the discussion of the end-group molecules on **LinLi01-10**. Our HTMs were divided into two groups: non-fluorinated ones (**LinLi01**/**02**/**08**/**09**/**10**) and fluorinated ones (**LinLi03**/**04**/**05**/**06**/**07**). In the group of non-fluorinated HTMs, it was noted that **LinLi01** and **LinLi02** with TPA-based end-groups exhibited similar HOMO energy levels ($E_{HOMO}=-5.17$, -5.13 eV), whereas **LinLi08**/**09**/**10** with carbazole- or phenothiazine-based end-groups showed the lower-lying E_{HOMO} of -5.19 eV~-5.33 eV. This indicated TPA possessed a stronger donor ability than Cbz and PTZ, which led to the red-shifted UV–vis absorptions. On the other hand, the fluorinated HTMs generally demonstrated the lower-lying E_{HOMO} of -5.21 eV~-5.29 eV because of the –F or $-CF_3$ moieties attached on TPA-based end-groups. Nevertheless, these E_{HOMO} values are still higher than those of **LinLi08**/**09** bearing Cbz groups ($E_{HOMO}=-5.30$, -5.33 eV), indicating carbazoles exhibited the poorest electron-donating ability among three kinds of end-groups. Next, by performing cyclic voltammetry to estimate the the highest occupied molecular orbital enregy (E_{HOMO}) of each molecule, we found their E_{HOMO} were all appropriately located between the E_{HOMO} of perovskite layer ($E_{HOMO}=-5.43$ eV) and Ag electrode ($E_{HOMO}=-4.20$ eV). This indicated **LinLi01-10** might extract holes effectively from the perovskite layer ($MAPbI_3$) and serve as potentially useful hole-transporting materials in PSC devices. Thermal gravimetric analysis (TGA) showed that three of the molecules bearing fluoro- or trifluoromethyl groups (**LinLi03**, **04**, **06**) had relatively lower decomposition temperatures ($T_d=367$, 332 and 368 °C). The measurement of differential scanning calorimetry (DSC) of partial HTMs has been carried out. However, it was found that **LinLi01**/**03**/**04**/**05**/**06**/**07**/**09**/**10** do not exhibit obvious/analytically valid glass transition temperatures (T_g), whereas the T_g

© 2023 Wiley-VCH GmbH

1861471x, 2023, 20, Downloaded from https://onlinelibrary.wiley.com/doi/10.1002/asia.202300681 by Ruhr-Universität Bochum, Wiley Online Library on [27/11/2023]. See the Terms and Conditions (https://onlinelibrary.wiley.com/terms-and-conditions) on Wiley Online Library for rules of use; OA articles are governed by the applicable Creative Commons License

spiro-OMeTAD was obtained (T_g = 126 °C). Additionally, the hole-mobility (μ_h) of each HTM was assessed by measuring their current density-voltage in the region of space-charge limited current (SCLC). The data revealed that **LinLi04** exhibited the highest hole mobility ($\mu_h = 6.08\times10^{-4}$ $cm^2V^{-1}s^{-1}$), whereas the molecule **LinLi07** without any –OMe, –SMe, or -*t*Bu substituents showed the lowest $\mu_h = 3.27\times10^{-4}$ $cm^2V^{-1}s^{-1}$.

Fabrication of perovskite solar cells (PSCs) incorporating **LLA01/02/03/04/06**, or **LinLi01-10** as hole-transport layer was carried out, respectively. Device fabrication procedures were detailed in Supporting Information. The data of PSCs photovoltaic performances were summarized in Table 4. PSCs employing **LLA01**, **02**, **03**, **04**, or **06** as HTM demonstrated poor power conversion efficiencies (PCEs = 0.1~2.0 %) owing to their low solubilities in chlorobenzene, which led to the occurrence of HTM recrystallization during the spin-coating process. On the other hand (**LinLi01-10**), it is worth noting that most devices were able to display > 10 % PCEs without any device oxidation process (except the PSCs based on **LinLi05/07/10**). In general, PSCs with the commmercial **spiro-OMeTAD** required 12 hours of oxidation to achieve the highest PCE of 20.43 %. Compared to PSCs with **LinLi01** bearing the typical dimethoxy substituents (–OMe), **LinLi02** carrying –SMe moieties gave even better PCEs (15.82 %). PSCs using **LinLi03** or **04** with additional fluorine atoms as HTM also provided improved PCEs (14.14 %; 17.54 %). This implied introduction of appropriate fluorine moieties to indolocarbazole may enhance the PCEs of perovskite-based solar cells devices. Moreover, **LinLi01/02/03/04/06/08/09**-based solar cells can be fabricated and treated with an oxidation-free process to show their PCEs of up to 17.5 % (**LinLi04**). Actually **LinLi04**-based devices exhibited comparable open-circuit voltage: V_{oc} = 1.01 V; short-circuit current: J_{sc} = 23.36 $mAcm^{-2}$; fill factor: *FF* = 76.07 % with the parameters obtained from **spiro-OMeTAD**-based PSCs (V_{oc} = 1.10 V; J_{sc} = 24.37 $mAcm^{-2}$; *FF* = 76.13 %). Based on above results, we may briefly conclude that significant improvements on PCEs of **LinLi01-10**-based devices had been observed after the EDOT moieties were inserted into molecular backbones as π-spacers (compared to **LLA01**, **02**, **03**, **04**, or **06**-based PSCs), presumably due to superior film formation.

Further, we performed the experiments of steady-state photoluminescence (PL) of **LinLi01-10** and the devices were fabicated as glass/perovskite/HTMs. In Figure 2, it was observed that **LinLi04/02/03/09**-based devices displayed relatively stronger PL quenching capabilities, indicating the above mentioned HTMs might be able to extract holes effectively at the interface between photoactive- and hole transporting-layers. Additionally, in Figure 2b and 2c, time-resolved photoluminescence (TRPL) spectra were also employed to investigate the charge extraction efficiency between the perovskite film and the HTMs. The PL lifetime of the films were fitted by a two-component exponential decay approach, as documented in the previous study.[21,22] Table S1 in the Supporting Information detailed the fitted parameters. The fast time constant, τ_1, corresponded to the charge extraction and recombination caused by surface traps (trap-assisted nonradiative recombination). Meanwhile, the slow time constant, τ_2, related to bimolecular recombination within the bulk perovskite (radiative recombination of free carriers). Impressively, the perovskite/HTMs demonstrated a shorter τ_1 lifetime than the standalone perovskite film, suggest-

Table 4. Evaluation of photovoltaic parameters of perovskite solar cells using **LinLi01-10** as HTMs (with two dopants: Li-TFSI/*t*-Bu-pyridine).[a,b]

HTMs		V_{oc} [V]	J_{sc} [$mAcm^{-2}$]	*FF* [%]	PCE [%]
LinLi01	best	0.95	20.64	57.04	11.17
	average	0.88 ± 0.06	20.21 ± 0.65	49.47 ± 8.89	8.92 ± 2.19
LinLi02	best	1.04	21.59	70.61	15.82
	average	1.03 ± 0.01	21.17 ± 0.28	64.46 ± 4.16	14.05 ± 1.00
LinLi03	best	1.00	21.99	64.11	14.14
	average	1.00 ± 0.02	21.53 ± 0.47	62.63 ± 1.70	13.46 ± 0.62
LinLi04	best	1.01	23.36	76.07	17.54
	average	1.00 ± 0.02	23.20 ± 0.18	73.72 ± 1.70	16.71 ± 0.53
LinLi05	best	0.83	19.19	53.77	8.52
	average	0.82 ± 0.01	19.26 ± 0.27	52.28 ± 1.06	8.25 ± 0.22
LinLi06	best	1.02	21.48	52.99	11.56
	average	0.90 ± 0.24	18.87 ± 1.61	39.94 ± 10.15	6.81 ± 3.09
LinLi07	best	0.94	17.25	44.30	7.12
	average	0.91 ± 0.02	15.60 ± 1.07	40.94 ± 4.16	5.82 ± 0.77
LinLi08	best	1.06	19.31	59.03	12.14
	average	1.04 ± 0.03	17.17 ± 1.66	55.53 ± 5.65	9.96 ± 1.40
LinLi09	best	1.02	21.73	60.49	13.31
	average	1.01 ± 0.03	21.31 ± 0.66	49.02 ± 6.61	10.53 ± 1.70
LinLi10	best	0.58	17.81	82.07	8.50
	average	0.84 ± 0.15	17.85 ± 1.00	53.93 ± 15.64	7.73 ± 0.52
spiro-OMeTAD	best	1.10	24.37	76.13	20.43
	average	1.09 ± 0.01	23.64 ± 0.49	75.69 ± 0.97	19.63 ± 0.55

[a] The statistical data were calculated based on 6 cells. [b] Forward scanning directions.

© 2023 Wiley-VCH GmbH

1861471x, 2023, 20, Downloaded from https://onlinelibrary.wiley.com/doi/10.1002/asia.202300681 by Ruhr-Universität Bochum, Wiley Online Library on [27/11/2023]. See the Terms and Conditions (https://onlinelibrary.wiley.com/terms-and-conditions) on Wiley Online Library for rules of use; OA articles are governed by the applicable Creative Commons License

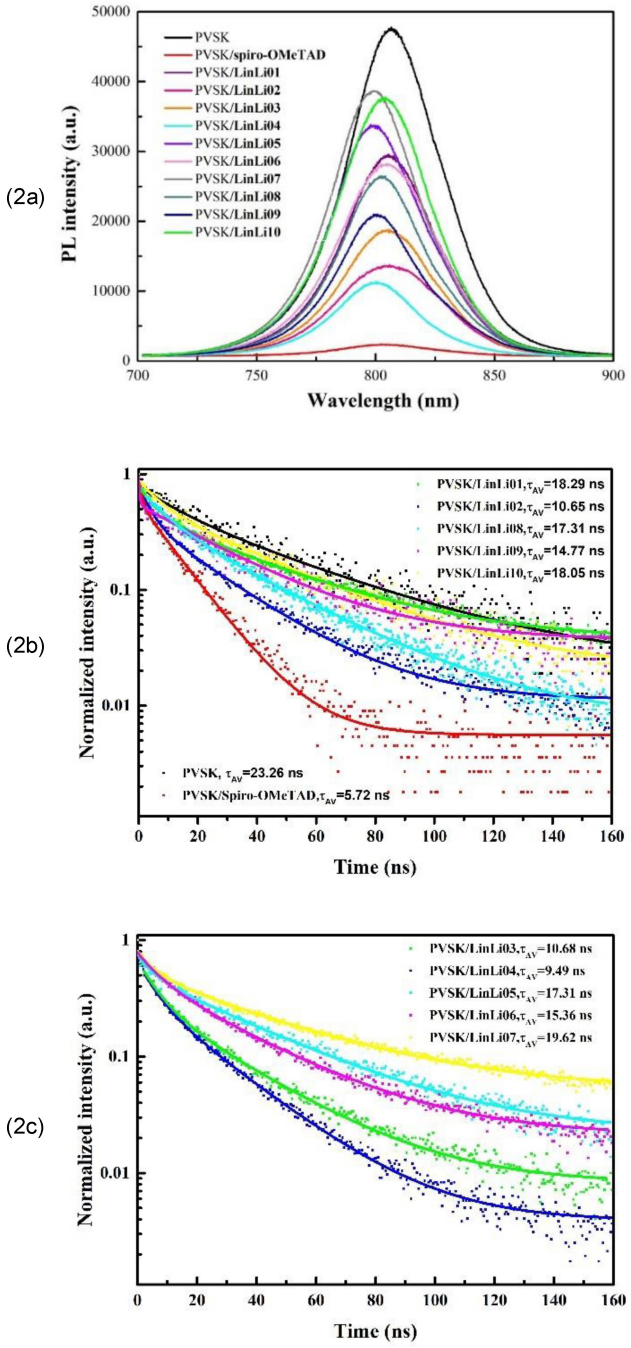

Figure 2. Steady-state PL (2a) and time-resolved photoluminescence (TRPL) (**2b**–**c**) spectra of the devices fabricated as glass/perovskite/HTM(**LinLi01-10**).

ing the HTMs' adeptness at efficient hole extraction. Notably, among the **LinLi** series of HTMs, the perovskite film coated with **LinLi04** exhibited the minimal lifetime with respect to other films. This denoted **LinLi04**'s superior ability in hole extraction, effectively curbing trap-induced non-radiative carrier recombination, thereby minimizing photocurrent losses in solar cells. Especially, the lifetime of **LinLi04** (with two –F moieties) is shorter than that of **LinLi03** (with one –F), which in turn is shorter than **LinLi01** (without –F). This suggested that the introduction of EDOT as π-spacer and -F moieties into end-groups effectively enhanced the interfacial charge recombination between the perovskite and HTM. Similarly, when comparing **LinLi06** with **LinLi01**, it's evident that the incorporation of $-CF_3$ moieties into end-groups offered comparable benefits. This observation aligned with the mobility results obtained from SCLC measurements in Table 3 and thier photovoltaic performances in Table 4.

To conduct a comprehensive investigation of the topological features of HTMs films spin-coated atop perovskite layers, atomic force microscopy (AFM) was employed to quantify the surface roughness of an assortment of HTM capping layers. As depicted in Figure 3, the perovskite-only film, lacking any HTMs, exhibited the highest root mean square roughness (Rq) value of 51.2 nm (refer to Figure 3a). Remarkably, the introduction of HTMs onto the perovskite films led to a substantial reduction in surface roughness, bringing it down to around 10 nm (Figures 3b–f). This observation aligned well with scanning electron microscopy (SEM) results presented in Figure 4, suggesting that HTMs facilitated the formation of a uniform and fully-covered capping layer on the underlying perovskite film. Besides, in Figure 4a, a top-view SEM image revealed a superior perovskite film characterized by well-organized grains, ranging in size from 300 to 700 nm. The recorded Rq values for various combinations were as follows: Perovskite/**spiro-OMeTAD** (7.06 nm), Perovskite/**LinLi04** (7.77 nm), Perovskite/**LinLi03** (7.97 nm), Per-

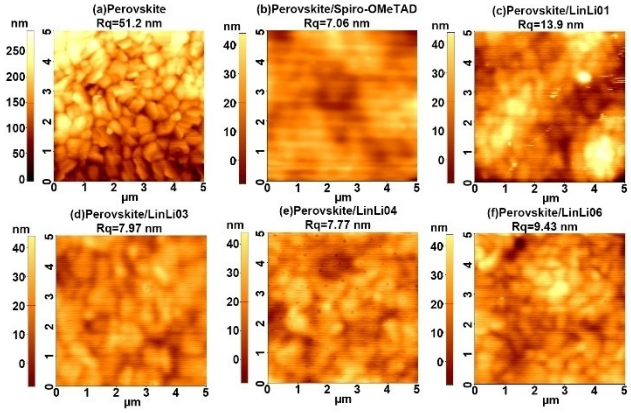

Figure 3. AFM images of top morphology of the perovskite films coated with (b) **spiro-OMeTAD**, (c) **LinLi01**, (d) **LinLi03**, (e) **LinLi04**, and (f) **LinLi06**.

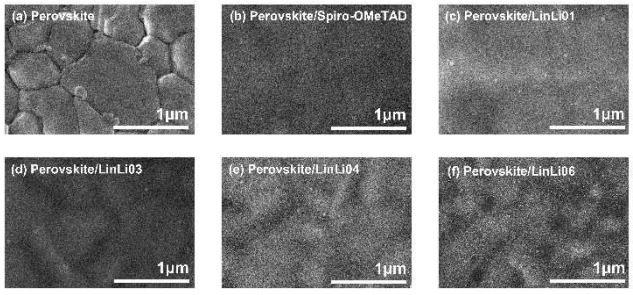

Figure 4. Top-view SEM images of (a) perovskite films and perovskite films coated with (b) **spiro-OMeTAD**, (c) **LinLi01**, (d) **LinLi03**, (e) **LinLi04**, and (f) **LinLi06**.

© 2023 Wiley-VCH GmbH

1861471x, 2023, 20, Downloaded from https://onlinelibrary.wiley.com/doi/10.1002/asia.202300681 by Ruhr-Universität Bochum, Wiley Online Library on [27/11/2023]. See the Terms and Conditions (https://onlinelibrary.wiley.com/terms-and-conditions) on Wiley Online Library for rules of use; OA articles are governed by the applicable Creative Commons License

ovskite/**LinLi06** (9.43 nm), and Perovskite/**LinLi01** (13.9 nm). Notably, the presence of –F/–CF_3 moieties in the end-groups contributed to smoother morphologies (Figures 4d–f), which are advantageous for efficient hole transfer and extraction at the interface. It's imperative to note that surface morphology and roughness exerted a significant impact on photovoltaic performances, particularly on the fill factors (FF).[23,24]

Conclusions

Indolocarbazole-containing oligoaryls were less investigated in the field of hole-transporting materials/perovskite solar cells. This work reported the facile preparation of 15 new indolocarbazole core-based small molecules (**LLA01/02/03/04/06** and **LinLi01-10**) utilizing Buchwald-Hartwig aminations or the π-conjugated organic materials-oriented direct C–H/C–Br couplings[25–28] as the key step, respectively. For the fabrication and evaluation of perovskite-based solar cells, we found that PSCs employing **LinLi01-10** as hole-transport layers generally exhibited superior photovoltaic performances than **LLA01/02/03/04/06**-based devices. Conclusively, introduction of EDOT as π-spacer and –F/–CF_3 moieties into end-groups created a new molecular design for indolocarbazole-based HTMs and led to considerably improved PCEs of their corresponding PSCs.

Acknowledgements

Financial support provided by the Ministry of Science and Technology (MOST), Taiwan (MOST 111-2113-M-008-008 and 108-2628-E-182-003-MY3), National Central University (NCU), Chang Gung University (QZRPD181) and Chang Gung Memorial Hospital, Linkou, Taiwan (CMRPD2M0041) are gratefully acknowledged. We also thank the instrument center (R&D office, NCU, MOST 110-2731-M-008-001) for the technical support of NMR and mass analysis.

Conflict of Interests

The authors declare no conflict of interest.

Data Availability Statement

The data that support the findings of this study are available in the supplementary material of this article.

Keywords: Indolocarbazole · Direct C–H Arylation · Molecular Design · Hole Transporting Materials · Perovskite Solar Cells

[1] G. W. Gribble, *J. Chem. Soc. Perkin Trans. 1* **2000**, 1045.
[2] M.-Z. Zhang, Q. Chen, G.-F. Yang, *Eur. J. Med. Chem.* **2015**, *89*, 421.
[3] J. Li, A. C. Grimsdale, *Chem. Soc. Rev.* **2010**, *39*, 2399.
[4] G. Sathiyan, E. K. T. Sivakumar, R. Ganesamoorthy, R. Thangamuthu, P. Sakthivel, *Tetrahedron Lett.* **2016**, *57*, 243.
[5] S. Omura, Y. Iwai, A. Hirano, A. Nakagawa, J. Awaya, H. Tsuchiya, Y. Takahashi, R. Masuma, *J. Antibiot.* **1977**, *30*, 275.
[6] G. Zhao, H. Dong, H. Zhao, L. Jiang, X. Zhang, J. Tan, Q. Meng, W. Hu, *J. Mater. Chem.* **2012**, *22*, 4409.
[7] Y. L. Wu, Y. N. Li, S. Gardner, B. S. Ong, *J. Am. Chem. Soc.* **2005**, *127*, 614.
[8] Y. N. Li, Y. L. Wu, S. Gardner, B. S. Ong, *Adv. Mater.* **2005**, *17*, 849.
[9] J. Y. Su, C. Y. Lo, C. H. Tasi, C. H. Chen, S. H. Chou, S. H. Liu, P. T. Chou, K. T. Wong, *Org. Lett.* **2014**, *16*, 3176.
[10] X.-H. Zhang, Z.-S. Wang, Y. Cui, N. Koumura, A. Furube, K. Hara, *J. Phys. Chem. C* **2009**, *113*, 13409.
[11] R. S. Mai, X. Y. Wu, Y. Jiang, Y. Y. Meng, B. Q. Liu, X. W. Hu, J. Roncali, G. F. Zhou, J. M. Liu, K. Kempa, J. W. Gao, *J. Mater. Chem. A* **2019**, *7*, 1539.
[12] B. Cai, X. Yang, X. Jiang, Z. Yu, A. Hagfeldt, L. Sun, *J. Mater. Chem. A* **2019**, *7*, 14835.
[13] I. Petrikyte, I. Zimmermann, K. Rakstys, M. Daskeviciene, T. Malinauskas, V. Jankauskas, V. Getautis, M. K. Nazeeruddin, *Nanoscale* **2016**, *8*, 8530.
[14] C. Lu, M. Aftabuzzaman, C. H. Kim, H. K. Kim, *Chem. Eng. J.* **2022**, *428*, 131108; S. H. Kang, C. Lu, H. Zhou, S. Choi, J. Kim, H. K. Kim, *Dyes Pigm.* **2019**, *163*, 734; C. Lu, I. T. Choi, J. Kim, H. K. Kim, *J. Mater. Chem. A* **2017**, *5*, 20263; S. D. Sung, M. S. Kang, I. T. Choi, H. M. Kim, H. Kim, M. P. Hong, H. K. Kim, W. I. Lee, *Chem. Commun.* **2014**, *50*, 14161; C. Lu, S. P. Hwang, K. W. Sung, C. H. Kim, H. K. Kim, *Dyes Pigm.* **2021**, *192*, 109432.
[15] Y.-C. Chang, K.-M. Lee, C.-C. Ting, C.-Y. Liu, *Mater. Chem. Front.* **2019**, *3*, 2041.
[16] P.-H. Lin, K.-M. Lee, C.-C. Ting, C.-Y. Liu, *J. Mater. Chem. A* **2019**, *7*, 5934.
[17] Y.-K. Peng, K.-M. Lee, C.-C. Ting, M.-W. Hsu, C.-Y. Liu, *J. Mater. Chem. A* **2019**, *7*, 24765.
[18] K.-M. Lu, K.-M. Lee, C.-H. Lai, C.-C. Ting, C.-Y. Liu, *Chem. Commun.* **2018**, *54*, 11495.
[19] a) C.-H. Tu, K.-M. Lee, J.-H. Chen, C.-H. Chiang, S.-C. Hsu, M.-W. Hsu, C.-Y. Liu, *Org. Chem. Front.* **2022**, *9*, 2821; b) C.-Y. Liu, P.-H. Lin, K.-M. Lee, *Chem. Rec.* **2021**, *21*, 3498.
[20] Please refer to the following papers for the synthesis of end-groups **3a–j** and **LinLi01-10** via optimized direct C–H/C–Br coupling reactions: a) Y.-C. Chang, K.-M. Lee, C.-H. Lai, C.-Y. Liu, *Chem. Asian J.* **2018**, *13*, 1510; b) J.-H. Chen, K.-M. Lee, C.-C. Ting, C.-Y. Liu, *RSC Adv.* **2021**, *11*, 8879.
[21] S. Ahn, W.-H. Chiu, H.-M. Cheng, V. Suryanarayanan, G. Chen, Y.-C. Huang, M.-C. Wu, K.-M. Lee, *Org. Electron.* **2023**, *120*, 106847.
[22] Z. Wu, M. Jiang, Z. Liu, A. Jamshaid, L. K. Ono, Y. Qi, *Adv. Energy Mater.* **2020**, *10*, 1903696.
[23] C. Lu, I. T. Choi, J. Kim, H. K. Kim, *J. Mater. Chem. A.* **2017**, *5*, 20263.
[24] K.-M. Lee, Y.-S. Huang, W.-H. Chiu, Y.-K. Huang, G. Chen, G. B. Adugna, S.-R. Li, F.-J. Lin, S.-I. Lu, H.-C. Hsieh, K.-L. Liau, C.-C. Huang, Y. Tai, Y.-T. Tao, Y.-D. Lin, *Adv. Funct. Mater.* **2023**, 2306367.
[25] L. Ackermann, R. Vicente, A. R. Kapdi, *Angew. Chem. Int. Ed.* **2009**, *48*, 9792.
[26] I. A. Stepek, K. Itami, *ACS Materials Lett.* **2020**, *2*, 951.
[27] a) A. Nitti, M. Signorile, M. Boiocchi, G. Bianchi, R. Po, D. Pasini, *J. Org. Chem.* **2016**, *81*, 11035; b) A. Nitti, G. Bianchi, R. Po, T. M. Swager, D. Pasini, *J. Am. Chem. Soc.* **2017**, *139*, 8788; c) G. Forti, R. M. Pankow, F. Qin, Y. Cho, B. Kerwin, I. Duplessis, A. Nitti, S. Jeong, C. Yang, A. Facchetti, D. Pasini, T. J. Marks, *Chem. Eur. J.* **2023**, *29*, e202300653; d) G. Bianchi, C. Carbonera, L. Ciammaruchi, N. Camaioni, N. Negarville, F. Tinti, G. Forti, A. Nitti, D. Pasini, A. Facchetti, R. M. Pankow, T. J. Marks, R. Po, *Solar RRL* **2022**, *6*, 2200643; e) A. Nitti, G. Forti, G. Bianchi, C. Botta, F. Tinti, M. Gazzano, N. Camaioni, R. Po, D. Pasini, *J. Mater. Chem. C* **2021**, *9*, 9302.
[28] C. Lu, M. Paramasivam, K. Park, C. H. Kim, H. K. Kim, *ACS Appl. Mater. Interfaces* **2019**, *11*, 14011.

Manuscript received: August 5, 2023
Revised manuscript received: August 30, 2023
Accepted manuscript online: September 11, 2023
Version of record online: September 20, 2023

© 2023 Wiley-VCH GmbH

1861471x, 2023, 20, Downloaded from https://onlinelibrary.wiley.com/doi/10.1002/asia.202300681 by Ruhr-Universität Bochum, Wiley Online Library on [27/11/2023]. See the Terms and Conditions (https://onlinelibrary.wiley.com/terms-and-conditions) on Wiley Online Library for rules of use; OA articles are governed by the applicable Creative Commons License